



Electrochemical evaluation of Abelson tyrosine-protein kinase 1 activity and inhibition by imatinib mesylate and danusertib



Victor C. Diculescu^{a,b,*}, Teodor A. Enache^b

^a Departamento de Engenharia Mecânica, Faculdade de Ciências e Tecnologia, Universidade de Coimbra, Rua Luís Reis Santos, 3030-788 Coimbra, Portugal

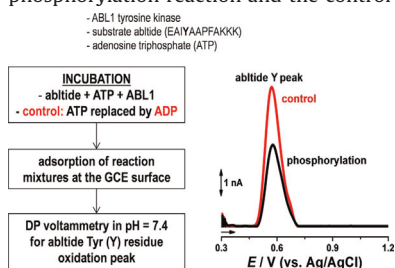
^b Laboratório de Electroanálise e Corrosão, Instituto Pedro Nunes, 3000-199 Coimbra, Portugal

HIGHLIGHTS

- Phosphorylation reactions by incubating ABL1, ATP and the substrate abltide.
- Reaction mixtures deposited at glassy carbon electrode.
- Activity reflected through variation of abltide tyrosine residue oxidation peak.
- Michaelis–Menten constant, turnover number and efficiency estimated.
- IC50 values estimated for inhibitors imatinib mesylate and danusertib.

GRAPHICAL ABSTRACT

Flowchart for the detection of ABL1-catalysed phosphorylation; DP voltammograms after the phosphorylation reaction and the control experiment.



ARTICLE INFO

Article history:

Received 12 May 2014

Received in revised form 12 June 2014

Accepted 15 June 2014

Available online 17 June 2014

Keywords:

Abelson tyrosine-protein kinase 1

Enzyme kinetics

Inhibition

Electrochemistry

Glassy carbon electrode

ABSTRACT

Abelson tyrosine-protein kinase 1 (ABL1) catalysed phosphorylation involves the addition of a phosphate group from ATP to the tyrosine residue on the substrate abltide. The phosphorylation reactions were carried out by incubating ABL1, ATP and the substrate abltide. Adsorption at the glassy carbon electrode surface in either reaction mixtures or control solutions, followed by differential pulse voltammetry in buffer allowed detection of the variation of abltide tyrosine residue oxidation peak reflecting the occurrence of the phosphorylation reaction. The effect of abltide, ATP and ABL1 concentrations as well as the time course of the phosphorylation reaction were studied. The influence of co-adsorption of ABL1, ATP and phosphorylated abltide was evaluated and the conditions for the electrochemical detection of ABL1-catalysed phosphorylation optimised. The Michaelis–Menten constant for abltide binding $K_M \sim 4.5 \mu\text{M}$, turnover number $k_{\text{cat}} \sim 11 \text{ s}^{-1}$ and enzyme efficiency $k_{\text{cat}}/K_M \sim 2.3 \text{ s}^{-1} \mu\text{M}^{-1}$ were calculated. The inhibition of ABL1 by imatinib mesylate and danusertib was also electrochemically investigated and IC50 values of 0.53 and 0.08 μM determined.

© 2014 Elsevier B.V. All rights reserved.

* Corresponding author at: Instituto Pedro Nunes, Laboratório de Electroanálise e Corrosão, Rua Pedro Nunes, 3000-199 Coimbra, Portugal. Tel.: +351 239 700 943; fax: +351 239 700 912.

E-mail address: victorcd@ipn.pt (V.C. Diculescu).

1. Introduction

Protein kinases are enzymes involved in signal transduction pathways, regulating a number of cellular functions such as cell growth, differentiation and cell death [1,2]. Kinases catalyse the transfer of the γ -phosphate from an ATP molecule to a tyrosine, serine or threonine residue on a substrate protein [3]. Any

deregulation in the signalling mechanism is a frequent cause of diseases [4,5] including cancer [2,4].

One of the most prominent examples is the Abelson tyrosine-protein kinase 1 (ABL1) [6], a cytoplasmic tyrosine kinase which mechanism of action is strictly regulated in healthy cells [7,8]. In chronic myeloid leukaemia (CML), the tyrosine kinase is constitutively activated [9] presenting enhanced uncontrolled activity. The ABL1 tyrosine kinase is responsible for the improved proliferation of cancer cells, turning this protein into a target for anticancer therapy [10].

Several synthetic kinase inhibitors were developed and their efficiency against various cancers described [11–13]. The leading compound in treatment of CML is imatinib mesylate [14], Scheme 1A, but resistance to imatinib has emerged as a major problem. Since ABL1 shares remarkable structural resemblance with other kinases, molecules such as danusertib [15], Scheme 1B, acting as dual ABL/Aurora kinase inhibitors possess enhanced activity against CML when compared with imatinib [16].

Due to the importance of kinases in the pathology of different diseases, assessing their activity and inhibition is significant from medical and biochemical points of view [17]. Highly sensitive, accurate, and reliable high throughput assays [18] for a variety of kinases have been developed. The general principle involves the detection of phosphorylation of specific oligopeptides selected through degenerate peptide libraries [19]. The main methodology is scintillation counting of radionuclides from ATP- γ - ^{32}P or ATP- γ - ^{35}S , after filter binding or electrophoresis and autoradiography [20], although detection with phospho-specific antibodies was reported as an alternative [21,22].

Also, fluorescence [23], surface plasmon resonance [24], electrophoretic [25] and chromatographic techniques [26] have been developed. Electroanalytical methods are sensitive and electrochemical biosensors for the detection of mutant ABL1-T315I, HER2/ErbB2, Rio1, Src-related kinases, EGFR and PKA catalysed phosphorylation reactions were described [27–31]. Most techniques involve labelling of ATP and detection of the labelled phosphate group after its transfer onto the corresponding substrate. Simple, adaptable and label-free assays to enable kinase activity detection are desirable [11].

The present study deals with the label-free electrochemical detection of ABL1 tyrosine kinase activity and inhibition, and uses previous reports which showed that phosphorylation of tyrosine leads to loss of the oxidation peak [32]. The protocol involving radiolabelled ATP molecules [33] was adapted for the electrochemical assay. The phosphorylation reactions were carried out by

incubating ABL1, ATP and the substrate abltide EAIYAAPFAKKK. Adsorption on the GCE the surface in incubated solution followed by differential pulse (DP) voltammetry in buffer allowed detection of the abltide Tyr residue oxidation peak. The decrease of abltide oxidation peak is consistent with the occurrence of the phosphorylation reaction. The conditions for the electrochemical detection of ABL1-catalysed phosphorylation were optimised, and Michaelis–Menten constant for abltide binding, turnover number and enzyme efficiency estimated. The inhibiting efficiencies of imatinib mesylate and danusertib were determined.

2. Experimental

2.1. Materials and reagents

ABL1 tyrosine kinase (specific activity 717–971 nmol min⁻¹ mg⁻¹), 4-morpholinepropanesulfonic acid (MOPS), glycerol-2-phosphate, MgCl₂, ethylene glycol-bis(2-aminoethylether)-N,N,N',N'-tetraacetic acid (EGTA), ethylenediaminetetraacetic acid (EDTA), dithiothreitol (DTT) from Sigma–Aldrich, substrate abltide from Enzo-Life Sciences, imatinib mesylate from Novartis Portugal and danusertib from Selleckchem were used without purification.

Kinase assay buffer (KAB) has been prepared by mixing 25 mM MOPS, pH 7.2, 12.5 mM glycerol-2-phosphate, 25 mM MgCl₂, 5 mM EGTA, and 2 mM EDTA. Just prior to use, DTT had been added to a final concentration of 0.25 mM.

Kinase dilution buffer (KDB) has been prepared by diluting 5-fold the kinase assay buffer with a solution of 0.05 $\mu\text{g mL}^{-1}$ bovine serum albumin (BSA) and 5% glycerol.

The stock solution of ABL1 (0.1 mg mL⁻¹) has been diluted with KDB to the desired concentration. 10 mM ATP has been prepared in KAB. The substrate was dissolved in deionized water to a final concentration of 750 μM . All solutions were stored at -20°C .

Microvolumes were measured using EP-10 and EP-100 Plus Motorized Microliter Pippettes (Rainin Instrument Co. Inc., Woburn, USA). The pH measurements were carried out with a Crison micropH 2001 pH-meter with an Ingold combined glass electrode. All experiments were done at room temperature ($25 \pm 1^\circ\text{C}$).

2.2. Voltammetric parameters and electrochemical cells

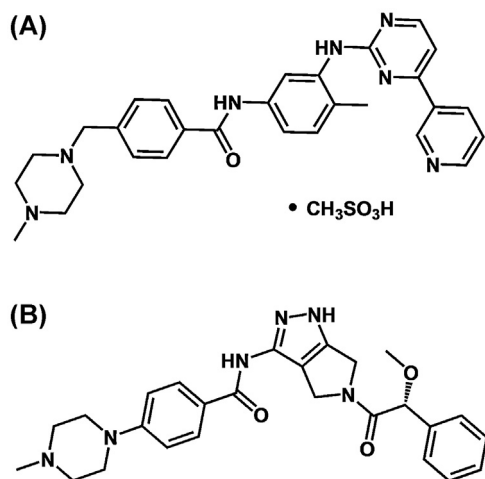
Voltammetric experiments were carried out using a Compact-Stat running with IviumSoft 2.124, Ivium Technologies, The Netherlands. The measurements were carried out using a three-electrode system in a 0.5 mL one-compartment electrochemical cell. A glassy carbon (GCE, $d = 1.0$ mm), a Pt wire, and a Ag/AgCl (3 M KCl) were used as working, auxiliary and reference electrodes, respectively.

The experimental conditions for differential pulse (DP) voltammetry were: pulse amplitude of 50 mV, pulse width of 100 ms and step potential of 2 mV for a scan rate of 5 mV s⁻¹. The DP voltammograms were recorded between +0.00 and +1.45 V.

The GCE was polished using diamond spray, particle size 3 μm (Kemet, UK) before each electrochemical experiment. After polishing, it was rinsed thoroughly with Milli-Q water. Following this mechanical treatment, the GCE was placed in buffer supporting electrolyte and differential pulse voltammograms were recorded until a steady state baseline voltammogram was obtained. This procedure ensured very reproducible experimental results.

2.3. Incubation procedure

The reaction mixtures were prepared in a pre-cooled test tube, where 10 μL of ABL1, 5 μL of substrate abltide, 5 μL ATP and 5 μL of



Scheme 1. Chemical structure of: (A) imatinib mesylate and (B) danusertib.

cold water were incubated at room temperature for the desired period of time.

For control experiments, the ATP in the incubation mixture was replaced by the same amount and concentration of ADP and the solution was incubated during 30 min.

For the detection of inhibitory effect of imatinib mesylate and danusertib the water in the incubation mixture has been replaced with 5 μL of inhibitor solution at different concentrations.

2.4. Electrochemical procedure

5 μL of the incubation mixture was placed on top of the GCE and allowed to freely adsorb during 3 min. Next, the electrode surface was washed in deionized water and placed in the electrochemical cell containing pH 7.4 0.1 M phosphate buffer where DP voltammetry was performed.

2.5. Acquisition and presentation of data

All voltammograms presented smoothed and baseline-corrected using an automatic function included in the IviumSoft version 2.124. This mathematical treatment improves the visualization and identification of peaks over the baseline without introducing any artefact.

Origin Pro 9.0 from OriginLab Corporation was used for the presentation and fitting of all the experimental data reported in this work.

3. Results and discussion

Phosphorylation reactions by ABL1 involve the addition of a phosphate group from ATP to a tyrosine (Tyr or Y) residue on substrate. Tyr is electroactive and its oxidation occurs with the transfer of electrons and protons from the hydroxyl group attached to the aromatic ring [32]. Phosphorylation of Tyr occurs at the same position and suppresses the electrochemical reaction, as previously demonstrated [32].

The phosphorylation reactions were carried out by incubating ABL1, ATP and the substrate abltide EAIYAAPFAKKK which contains the Tyr(Y) residue. After an appropriate incubation period, adsorption of the reaction mixture on the GCE the surface was carried out. Next, the electrode was washed with deionised water to remove the unbound molecules and placed into the electrochemical cell containing only phosphate buffer pH 7.4. The DP voltammetry was performed for detection of the abltide Tyr residue oxidation peak. The decrease of abltide oxidation peak is consistent with the decrease of the abltide concentration after the phosphorylation reaction. For control experiments, the ATP in the reaction mixture is replaced by ADP and no phosphorylation takes place, allowing the occurrence of high abltide Tyr residue oxidation peak.

3.1. Electrochemical characterisation of abltide

The influence of the reaction mixture components on the abltide Tyr residue oxidation peak was studied. DP voltammograms were recorded in pH 7.4 after adsorption during 3 min in a 5 μM abltide solution in the absence and presence of either 0.10 $\mu\text{g mL}^{-1}$ ABL1 or 100 μM ATP.

In the absence of ABL1 and ATP the voltammogram showed one main anodic peak at $E_{\text{pa}} = +0.57$ V due to the oxidation of tyrosine residues. The presence of ABL1 did not influence the abltide oxidation peak (not shown). Contrary, ATP and abltide co-adsorbed at the GCE surface, and a small positive displacement (~ 5 mV) of abltide Tyr residue oxidation peak was observed.

The electroanalytical determination of abltide has been carried out by DPV in pH 7.4 after adsorption during 3 min in solutions of

different concentrations in the presence of 100 μM ATP, Fig. 1A. The peak correspondent to Tyr residues in the abltide sequence increased with increasing concentration. Linearity has been observed up to 10 μM abltide, Fig. 1B, following the Eq (1):

$$I_{\text{pa}} (\text{nA}) = 0.99 + 0.65C_{\text{abltide}} (\mu\text{M}) (R^2 = 0.985) \quad (1)$$

For higher concentration, GCE saturation effects were observed, Fig. 1.

3.2. Electrochemical characterisation of ABL1 activity

The DP voltammogram recorded in pH 7.4 after adsorption in reaction mixture containing 5 μM abltide, 0.10 $\mu\text{g mL}^{-1}$ ABL1 and 100 μM ATP incubated during 15 min, showed a small peak specific to abltide oxidation, Fig. 2A. On the control voltammogram, recorded for a similar reaction mixture but in which ATP has been replaced by ADP, Fig. 2A, a high abltide oxidation peak occurred. This behaviour is consistent with the decrease of the concentration of abltide available for oxidation after the phosphorylation reaction. The occurrence of a small abltide oxidation peak is attributed to abltide molecules that were not phosphorylated.

The ABL1-catalysed phosphorylation is dependent on reagents concentrations. The effect of abltide, ATP and ABL1 concentrations were evaluated in order to determine the optimum conditions for studying the time-course of the phosphorylation reaction and inhibiting capacity of imatinib mesylate and danusertib.

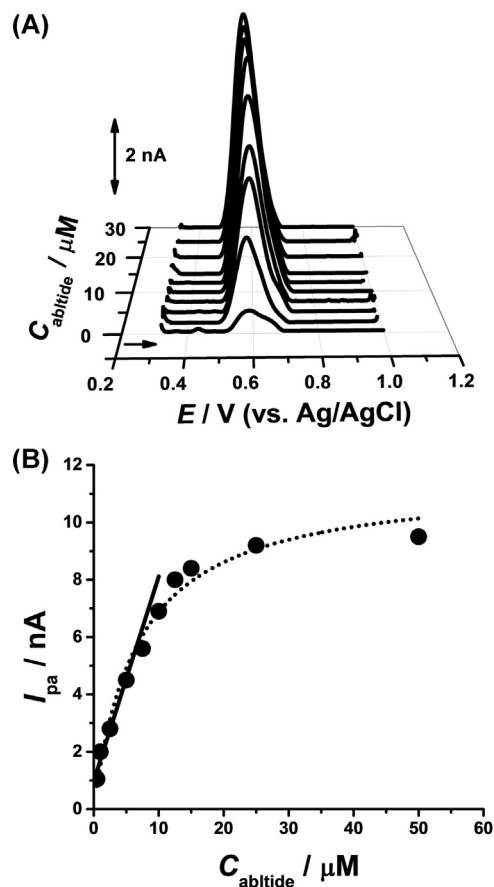


Fig. 1. (A) DP voltammograms base-line corrected in pH 7.4 after adsorption during 3 min in solutions of different abltide concentrations in the presence of 100 μM ATP; (B) Dependence of I_{pa} of abltide on abltide concentration in the presence of 100 μM ATP.

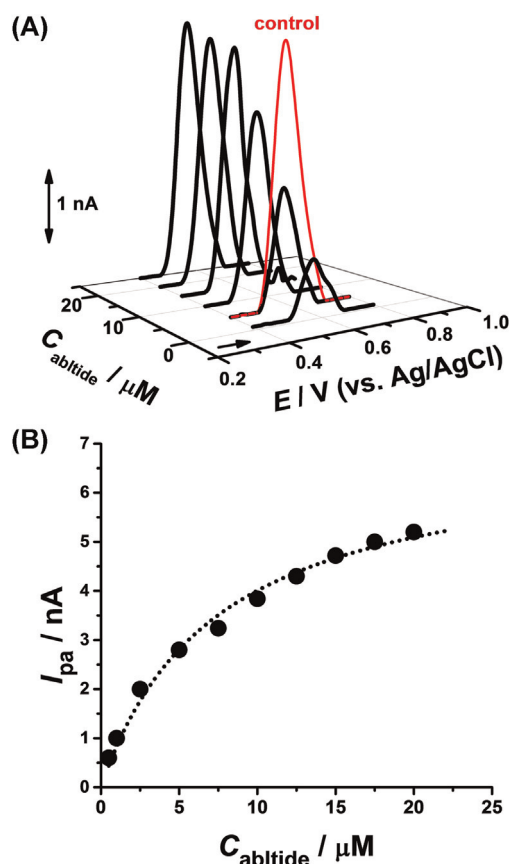


Fig. 2. (A) DP voltammograms base-line corrected in pH 7.4 after adsorption for 3 min in reaction mixtures (black curves) containing different abltide concentrations, 0.10 $\mu\text{g mL}^{-1}$ ABL1 and 100 μM ATP incubated during 15 min, and (red curve) control experiment. (B) Dependence of I_{pa} of abltide phosphorylated during 15 min in the presence of 0.10 $\mu\text{g mL}^{-1}$ ABL1 and 100 μM ATP vs. abltide concentration. (For interpretation of the references to color in this figure legend, the reader is referred to the web version of this article.)

3.2.1. Abltide concentration effect

In order to optimise the conditions for the electrochemical evaluation of ABL1 activity, DPV was performed for reaction mixtures containing different concentrations of abltide, 0.10 $\mu\text{g mL}^{-1}$ ABL1 and 100 μM ATP incubated during 15 min, Fig. 2A. The abltide concentration was varied from 0.5 to 20.0 μM . Between experiments the GCE surface was always cleaned. The oxidation peak of Tyr residue increased with increasing abltide concentration, reaching constant values for $C_{abltide} > 10 \mu\text{M}$, Fig. 2B. Non-linear regression was applied to the experimental data points using the adapted Michaelis–Menten Eq. (2):

$$I_{pa} = \frac{I_{max} \times C_{abltide}}{(K_M^{app} + C_{abltide})} \quad (2)$$

allowing $K_M^{app} = 6.93 \pm 0.69 \mu\text{M}$ and $I_{max} = 6.75 \pm 0.19 \text{ nA}$. This experiment shows that increasing the abltide concentration, the quantity of substrate that did not undergo phosphorylation reaches constant values. Although the I_{max} is smaller than the maximum current on the abltide calibration curve, Fig. 2B, electrode saturation effects due to the co-adsorption of both phosphorylated and not-phosphorylated forms of abltide are responsible for this effect. In order to avoid limitations imposed by GCE saturation, all experiments were carried out for $C_{abltide} = 5.0 \mu\text{M}$, below the GCE saturation limit, Fig. 2B.

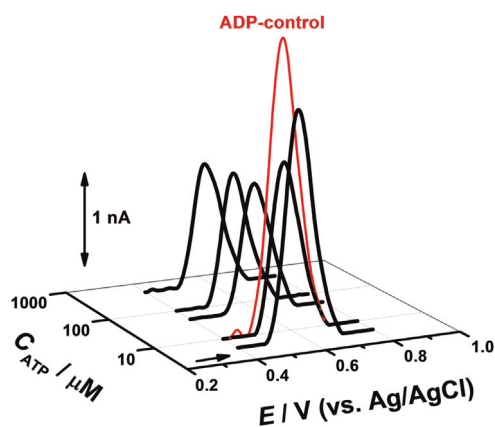


Fig. 3. DP voltammograms base-line corrected in pH 7.4 after adsorption for 3 min in reaction mixtures (black curves) containing 5 μM abltide, 0.10 $\mu\text{g mL}^{-1}$ ABL1 and different concentration of ATP incubated during 15 min, and (red curve) control experiment. (For interpretation of the references to color in this figure legend, the reader is referred to the web version of this article.)

3.2.2. ATP concentration effect

The influence of ATP on the phosphorylation reaction was also studied. DP voltammograms were recorded in buffer pH 7.4 after adsorption in reaction mixtures containing 5 μM abltide, 0.10 $\mu\text{g mL}^{-1}$ ABL1 and different concentration of ATP incubated during 15 min, Fig. 3. The abltide oxidation peak decreased with increasing ATP concentration and constant values were reached for $C_{ATP} > 10 \mu\text{M}$.

3.2.3. ABL1 concentration effect

For the evaluation of the enzyme concentration effect, adsorption was performed in reaction mixtures containing 5 μM abltide, different concentrations of ABL1 and 100 μM ATP incubated during 15 min, Fig. 4A. The abltide oxidation peak gradually decreased with increasing enzyme concentration up to 1 $\mu\text{g mL}^{-1}$, Fig. 4B. Control experiments with ADP in the presence of high enzyme concentrations showed high currents.

By using the abltide calibration curve Eq. (1), the recorded currents were transformed into concentration values, and consequently quantity of phosphorylated abltide (p-abltide), Fig. 4C. Enzyme saturation occurred for $m_{ABL1} > 10 \text{ ng}$. For $m_{ABL1} < 10 \text{ ng}$ linearity was observed with a slope of 20.03 pmol ng^{-1} and standard deviation (S.D.) of 16.28 pmol . The detection limit for the phosphorylation activity of ABL1 was calculated from $\text{LOD} = 3 \times \text{S.D.} \times (\text{sensitivity})^{-1}$ to be $\text{LOD} = 2.43 \text{ ng}$ (0.098 $\mu\text{g mL}^{-1}$).

3.2.4. Phosphorylation time effect

The time course of the phosphorylation reaction was investigated. The adsorption was carried out in reaction mixtures containing 5 μM abltide, 0.20 $\mu\text{g mL}^{-1}$ ABL1 and 100 μM ATP incubated during different times. Between experiments, the GCE surface was always cleaned. A progressive decrease of the abltide oxidation peak occurred up to 15 min of incubation, Fig. 5A. For lower ABL1 concentrations, higher time-dependent abltide oxidation peaks were obtained, Fig. 5B.

Using the abltide calibration curve, the concentrations of non-phosphorylated abltide were calculated for different incubation times, Fig. 5C. Nonlinear regression analysis was applied to the progression curves using the solution of the integrated Michaelis–Menten equation [34]:

$$S(t) = S_f + K_M \times W \left\{ \frac{S_0 - S_f}{K_M} \exp \left[\frac{S_0 - S_f - C_{ABL1} \times k_{cat} \times t}{K_M} \right] \right\} \quad (3)$$

where $S(t)$ is the substrate concentration function of incubation

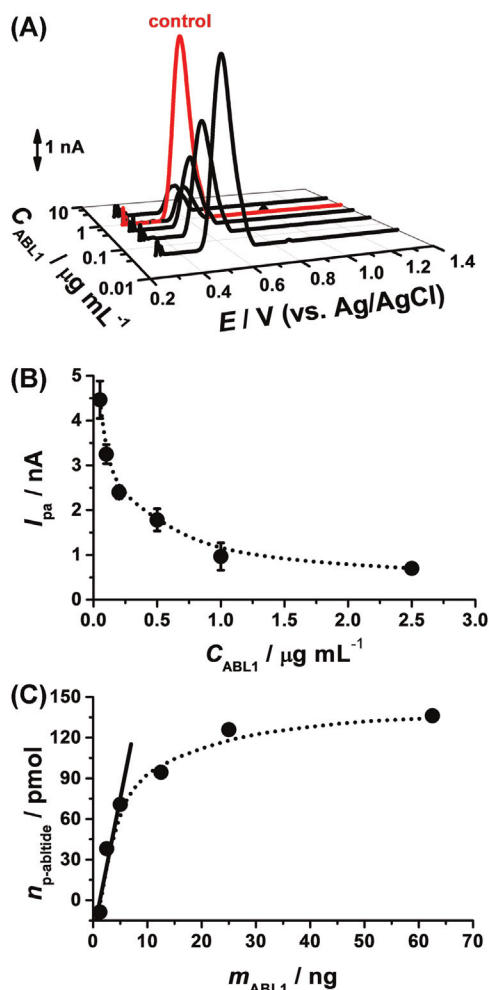


Fig. 4. (A) DP voltammograms base-line corrected recorded in pH 7.4 after adsorption for 3 min in reaction mixtures (black curves) containing 5 μM abltide, different concentrations of ABL1 and 100 μM ATP incubated during 15 min, and (red curve) control experiment with 100 μM ADP. Dependence of: (B) I_{pa} of abltide on C_{ABL1} concentration and (C) $n_{p-abltide}$ function of m_{ABL1} for reaction mixtures containing 5 μM abltide, different concentrations of ABL1 and 100 μM ATP incubated during 15 min. (For interpretation of the references to color in this figure legend, the reader is referred to the web version of this article.)

time t , $S_0=5\mu\text{M}$ the initial substrate concentration, S_f the concentration of residual unreacted substrate, K_M the Michaelis–Menten constant, k_{cat} the turnover number, and $W(x)$ is the Lambert function defined as $W(x)=x \exp[-W(x)]$. The S_f value was calculated from the last data points corresponding to 30 min incubation time.

Fitting the experimental results with Eq. (3), Table 1, $K_M \sim 4.5\mu\text{M}$, the average turnover number $k_{cat} \sim 11\text{ s}^{-1}$ and enzyme efficiency or specificity constant $k_{cat}/K_M \sim 2.3\text{ s}^{-1}\mu\text{M}^{-1}$ can be determined. For these calculations enzymes concentrations of 0.74 and 1.48 nM were based on an estimated 135 kDa molecular mass of ABL1.

3.3. Electrochemical evaluation of ABL1 inhibitors

The inhibiting efficiency of imatinib mesylate and danusertib, Scheme 1, two synthetic ATP-semi competitive inhibitors of ABL1 was evaluated. The experiments were carried out for reaction mixtures containing 5 μM abltide, 0.10 $\mu\text{g mL}^{-1}$ ABL1 and 100 μM ATP incubated during 15 min in the presence of different concentrations of inhibitors.

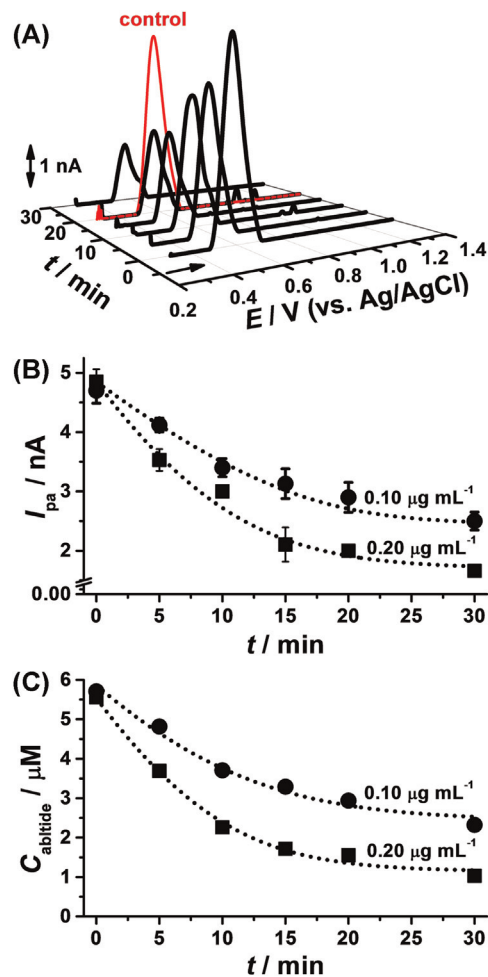


Fig. 5. (A) DP voltammograms base-line corrected recorded in pH 7.4 after adsorption for 3 min in reaction mixtures (black curves) containing 5 μM abltide, 0.20 $\mu\text{g mL}^{-1}$ ABL1 and 100 μM ATP during different times, and (red curve) control experiment with 100 μM ADP. Dependence of: (B) I_{pa} of abltide and (C) $C_{abltide}$ on phosphorylation time t for reaction mixtures containing 5 μM abltide, 0.10 or 0.20 $\mu\text{g mL}^{-1}$ ABL1 and 100 μM ATP incubated during different times. (For interpretation of the references to color in this figure legend, the reader is referred to the web version of this article.)

For low inhibitor concentration, the phosphorylation reaction proceeds and the DP voltammogram recorded for reaction mixtures in the presence of 0.3 μM imatinib mesylate showed a small abltide oxidation peak at $E_{pa}=+0.57\text{ V}$, Fig. 6A. The control experiment where no phosphorylation is expected showed a high abltide oxidation peak. Nevertheless, the peak at $E_{pa}=+0.78\text{ V}$ specific to the oxidation of imatinib molecules reflected the co-adsorption of inhibitor at the GCE surface, Fig. 6A.

For high inhibitor concentration, the phosphorylation reaction is blocked. Indeed, the DP voltammogram recorded for reaction mixtures in the presence of 2.5 μM imatinib mesylate, showed abltide oxidation peak with current values close to those obtained for control experiment, Fig. 6B. Higher imatinib oxidation peak can

Table 1
Michaelis–Menten constant, turnover number and enzyme efficiency calculated by non-linear regression of progress curves in Fig. 5 for two enzyme concentrations.

C_{ABL1} (nM)	K_M (μM)	k_{cat} (s^{-1})	k_{cat}/K_M^{app} ($\text{s}^{-1}\mu\text{M}^{-1}$)
0.74	4.24 ± 0.25	11.13 ± 0.43	2.63
1.48	4.89 ± 0.31	10.78 ± 0.46	2.21

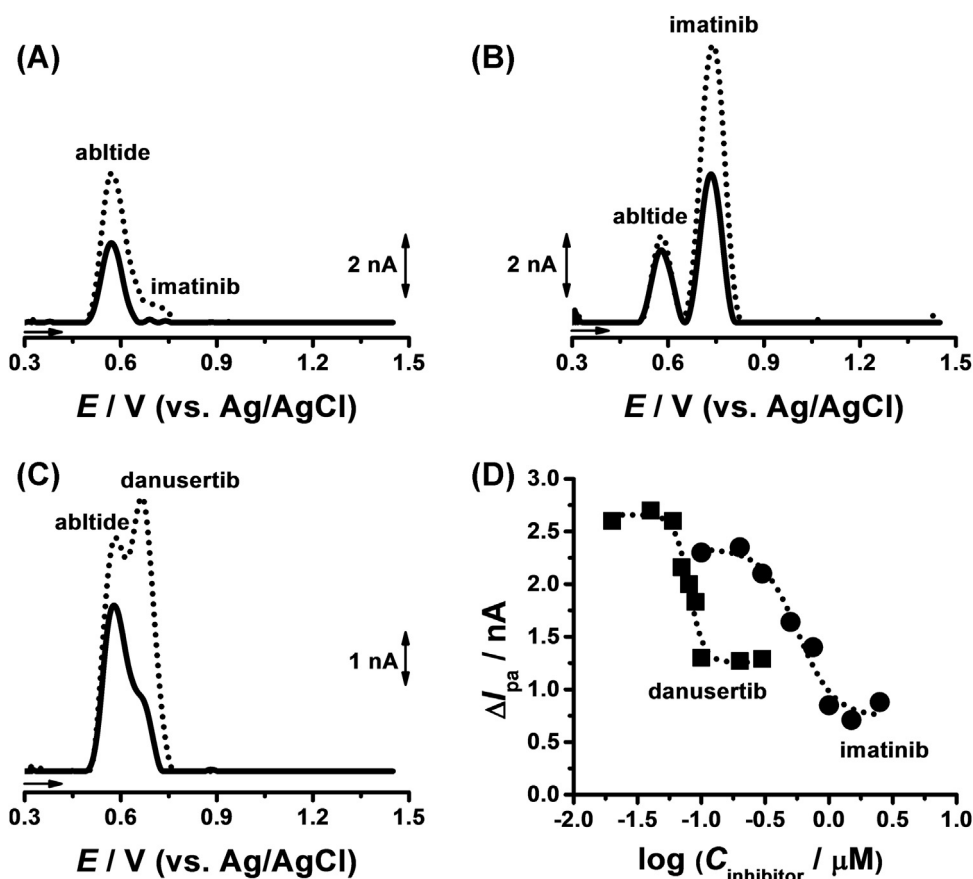


Fig. 6. DP voltammograms base-line corrected recorded in pH 7.4 after adsorption for 3 min in reaction mixtures (black curves) containing 5 μM abltide, 0.10 $\mu\text{g mL}^{-1}$ ABL1, 100 μM ATP incubated during 15 min in the presence of: (A) 0.3, (B) 1.0 μM imatinib, (C) 0.2 μM danusertib, and (dotted curves) control experiments. (D) Dependence of the difference in current ΔI_{pa} vs. $\log(C_{\text{inhibitor}})$, recorded for inhibited reaction mixtures and control solutions for: (●) imatinib mesylate and (■) danusertib.

be observed due to the co-adsorption of the inhibitor at the GCE surface.

Also, experiments were performed for the determination of danusertib inhibiting efficiency and a similar behaviour was observed, Fig. 6C.

Comparing the results in Fig. 6A–C, it is observed that the oxidation peak of abltide is strongly influenced by the co-adsorption of inhibitor at the GCE surface. High inhibitor concentrations diminish the abltide oxidation peak. Yet, the data show that the difference (ΔI_{pa}) between the abltide peak current recorded for the control solution and the abltide peak current registered for the inhibited reaction mixture is dependent on the inhibitor concentration and decreased with increasing inhibitor concentration. The value ΔI_{pa} was chosen as analytical signal for the determination of the inhibiting capacity of compounds.

The plots of ΔI_{pa} as a function of the logarithm of inhibitors concentration present sigmoidal shape for both imatinib and danusertib, Fig. 6D. The inhibitor concentration required to produce 50% inhibition of the enzymatic reaction at a specific peptide concentration, IC_{50} , was obtained by a non-linear fit of the experimental data using the dose-response equation:

$$\Delta I_{pa} = \Delta I_{\min} + (\Delta I_{\max} - \Delta I_{\min}) / (1 + 10^{(\log IC_{50} - C)p}) \quad (4)$$

where ΔI_{\min} and ΔI_{\max} are the minimum and maximum current difference, respectively, and p is the Hill slope that describes the inclination of the linear part of the plot.

The experimental data were fitted with the dose-response Eq. (4). IC_{50} values for imatinib mesylate and danusertib were estimated to be 0.53 and 0.08 μM , respectively.

4. Conclusions

The ABL1 tyrosine kinase-catalysed phosphorylation reaction was studied using a glassy carbon electrode and differential pulse voltammetry. The phosphorylation reactions were carried out by incubating ABL1, ATP and the substrate abltide. Adsorption on the glassy carbon electrode surface in either incubated reaction mixtures or control solutions, followed by differential pulse voltammetry in buffer allowed detection of the abltide tyrosine residues oxidation peak. It has been shown that the phosphorylation of the tyrosine residue on the substrate abltide leads to the decrease of the abltide oxidation peak.

The effect of abltide, ATP and ABL1 concentrations were investigated. It was demonstrated that the co-adsorption of ATP and phosphorylated abltide strands at the electrode surface directly influences the detection of the phosphorylation reaction. The conditions for the electrochemical detection of ABL1-catalysed phosphorylation were optimised.

The time course of the phosphorylation reaction was also studied. By following the time-dependent variation of abltide oxidation peak, Michaelis–Menten constant for abltide binding $K_M \sim 4.5 \mu\text{M}$, turnover number $k_{\text{cat}} \sim 11 \text{ s}^{-1}$ and enzyme efficiency $k_{\text{cat}}/K_M \sim 2.3 \text{ s}^{-1} \mu\text{M}^{-1}$ were calculated.

Also, the inhibition of ABL1 by imatinib mesylate and danusertib was evaluated. IC_{50} values were estimated to be 0.53 and 0.08 μM , respectively.

The present study provides a simple and fast methodology for the detection and evaluation of ABL1 tyrosine kinase activity and inhibition.

Acknowledgements

Financial support from: Fundação para a Ciência e Tecnologia (FCT), Post-Doctoral Grant SFRH/BPD/80195/2011 (T.A. Enache), projects PTDC/SAU-BEB/104643/2008, PTDC/DTP-FTO/0191/2012, PEst-C/EME/UI0285/2013 and CENTRO-07-0224-FEDER-002001 (MT4MOBI) (co-financed by the European Community Fund FEDER), FEDER funds through the program COMPETE–Programa Operacional Factores de Competitividade is gratefully acknowledged.

References

- [1] P. Cohen, The origins of protein phosphorylation, *Nat. Cell Biol.* 4 (2002) E127–E130.
- [2] J. Brognard, T. Hunter, Protein kinase signaling networks in cancer, *Curr. Opin. Genet. Dev.* 21 (2011) 4–11.
- [3] J.A. Ubersax, J.E. Ferrell Jr., Mechanisms of specificity in protein phosphorylation, *Nat. Rev. Mol. Cell Biol.* 8 (2007) 530–541.
- [4] I. Shchemelinin, L. Sefc, E. Necas, Protein kinases, their function and implication in cancer and other diseases, *Folia Biol. (Praha)* 52 (2006) 81–100.
- [5] L.K. Chico, L.J. Van Eldik, D.M. Watterson, Targeting protein kinases in central nervous system disorders, *Nat. Rev. Drug Discov.* 8 (2009) 892–909.
- [6] J. Colicelli, ABL tyrosine kinases: evolution of function, regulation, and specificity, *Sci. Signal.* 3 (2010) re6.
- [7] O. Hantschel, Structure, regulation, signaling, and targeting of abl kinases in cancer, *Genes Cancer* 3 (2012) 436–446.
- [8] Y. Shaul, c-Abl: activation and nuclear targets c-Abl: activation and nuclear targets, *Cell Death Differ.* 7 (2000) 10–16.
- [9] S. Medves, J.-B. Demoulin, Tyrosine kinase gene fusions in cancer: translating mechanisms into targeted therapies, *J. Cell. Mol. Med.* 16 (2012) 237–248.
- [10] M. Warmuth, S. Kim, X.J. Gu, G. Xia, F. Adrian, Ba/F3 cells and their use in kinase drug discovery, *Curr. Opin. Oncol.* 19 (2007) 55–60.
- [11] S. Madhusudan, T.S. Ganesan, Tyrosine kinase inhibitors in cancer therapy, *Clin. Biochem.* 37 (2004) 618–635.
- [12] E.G. Pereira, M.A.M. Moreira, E.R. Caffarena, Molecular interactions of c-ABL mutants in complex with imatinib/nilotinib: a computational study using linear interaction energy (LIE) calculations, *J. Mol. Model.* 18 (2012) 4333–4341.
- [13] D. White, V. Saunders, A.B. Lyons, S. Branford, A. Grigg, L.B. To, T. Hughes, In vitro sensitivity to imatinib-induced inhibition of ABL kinase activity is predictive of molecular response in patients with de novo CML, *Blood* 106 (2005) 2520–2526.
- [14] V.C. Diculescu, M. Vivan, A.M. Oliveira Brett, Voltammetric behavior of antileukemia drug glivec. Part I – electrochemical study of glivec, *Electroanalysis* 18 (2006) 1800–1807.
- [15] O.M. Popa, V.C. Diculescu, Electrochemical and spectrophotometric characterisation of protein kinase inhibitor and anticancer drug danusertib, *Electrochim. Acta* 112 (2013) 486–492.
- [16] S. Schenone, O. Bruno, M. Radi, M. Botta, New insights into small-molecule inhibitors of Bcr-Abl, *Med. Res. Rev.* 31 (1) (2010) 1–41.
- [17] A.D. Powers, S.P. Palecek, Protein analytical assays for diagnosing, monitoring, and choosing treatment for cancer patients, *J. Healthc. Eng.* 3 (2012) 503–533.
- [18] J. Cottom, G. Hofmann, B. Siegfried, J.S. Yang, H. Zhang, T. Yi, T.F. Ho, C. Quinn, D. Y. Wang, K. Johanson, R.S. Ames, H. Li, Assay development and high-throughput screening of small molecular c-Abl kinase activators, *J. Biomol. Screen.* 16 (2011) 53–64.
- [19] Z. Songyang, K.L. Carraway, M.J. Eck, S.C. Harrison, R.A. Feldman, M. Mohammadi, J. Schlessinger, S.R. Hubbard, D.P. Smith, C. Eng, M.J. Lorenzo, B.A.J. Ponder, B.J. Mayer, L.C. Cantley, Catalytic specificity of protein-tyrosine kinases is critical for selective signaling, *Nature* 373 (1995) 536–539.
- [20] J.E. Casnellie, Assay of protein kinases using peptides with basic residues for phosphocellulose binding, *Method. Enzymol.* 200 (1991) 115–120.
- [21] S. Panse, L.Y. Dong, A. Burian, R. Carus, M. Schutkowski, U. Reimer, J. Schneider-Mergener, Profiling of generic anti-phosphopeptide antibodies and kinases with peptide microarrays using radioactive and fluorescence-based assays, *Mol. Divers.* 8 (2004) 291–299.
- [22] J.Y. Wu, D.J. Yang, L.S. Angelo, S. Kohanim, R. Kurzrock, Molecular imaging of Bcr-Abl phosphokinase in a xenograft model, *Mol. Cancer Ther.* 8 (2009) 703–710.
- [23] M.C. Morris, Fluorescent biosensors – probing protein kinase function in cancer and drug discovery, *Biochim. Biophys. Acta* 1834 (2013) 1387–1395.
- [24] T. Mori, K. Inamori, Y. Inoue, X. Han, G. Yamanouchi, T. Niidome, Y. Katayama, Evaluation of protein kinase activities of cell lysates using peptide microarrays based on surface plasmon resonance imaging, *Anal. Biochem.* 375 (2008) 223–231.
- [25] D. Wu, E. Nair-Gill, D.A. Sher, L.L. Parker, J.M. Campbell, M. Siddiqui, W. Stock, S. J. Kron, Assaying Bcr-Abl kinase activity and inhibition in whole cell extracts by phosphorylation of substrates immobilized on agarose beads, *Anal. Biochem.* 347 (2005) 67–76.
- [26] H. Chen, E. Adams, A. Van Schepdael, LC–ESI–MS method for the monitoring of Abl1 tyrosine kinase, *J. Chromatogr. B* 897 (2012) 17–21.
- [27] K. Kerman, H.-B. Kraatz, Electrochemical detection of protein tyrosine kinase-catalysed phosphorylation using gold nanoparticles, *Biosens. Bioelectron.* 24 (2009) 1484–1489.
- [28] K. Kerman, H. Song, J.S. Duncan, D.W. Litchfield, H.-B. Kraatz, Peptide biosensors for the electrochemical measurement of protein kinase activity, *Anal. Chem.* 80 (2008) 9395–9401.
- [29] S. Martic, M. Labib, H.B. Kraatz, Enzymatically modified peptide surfaces: towards general electrochemical sensor platform for protein kinase catalyzed phosphorylations, *Analyst* 136 (2011) 107–112.
- [30] K. Kerman, M. Vestergaard, E. Tamiya, Label-free electrical sensing of small-molecule inhibition on tyrosine phosphorylation, *Anal. Chem.* 79 (2007) 6881–6885.
- [31] Y. Katayama, S. Sakakihara, M. Maeda, Electrochemical sensing for the determination of activated cyclic AMP-dependent protein kinase, *Anal. Sci.* 17 (2001) 17–19.
- [32] O.M. Popa, V.C. Diculescu, Electrochemical oxidation mechanism of phosphotyrosine at a glassy carbon electrode, *J. Electroanal. Chem.* 689 (2013) 216–222.
- [33] <http://www.sigmaaldrich.com/content/dam/sigma-aldrich/docs/Sigma/Data-sheet/10/a0608dat.pdf>
- [34] S. Schnell, P.K. Maini, A century of enzyme kinetics: reliability of the Km and Vmax estimates, *Comment. Theor. Biol.* 8 (2003) 169–187.